Supporting Information: Symmetry-related Proton Transfer Pathways in Respiratory Complex I

Andrea Di Luca, Ana P. Gamiz-Hernandez, Ville R. I. Kaila*
Department Chemie, Technische Universität München, Lichtenbergstr. 4, Garching, Germany.
*Corresponding author: ville.kaila@ch.tum.de

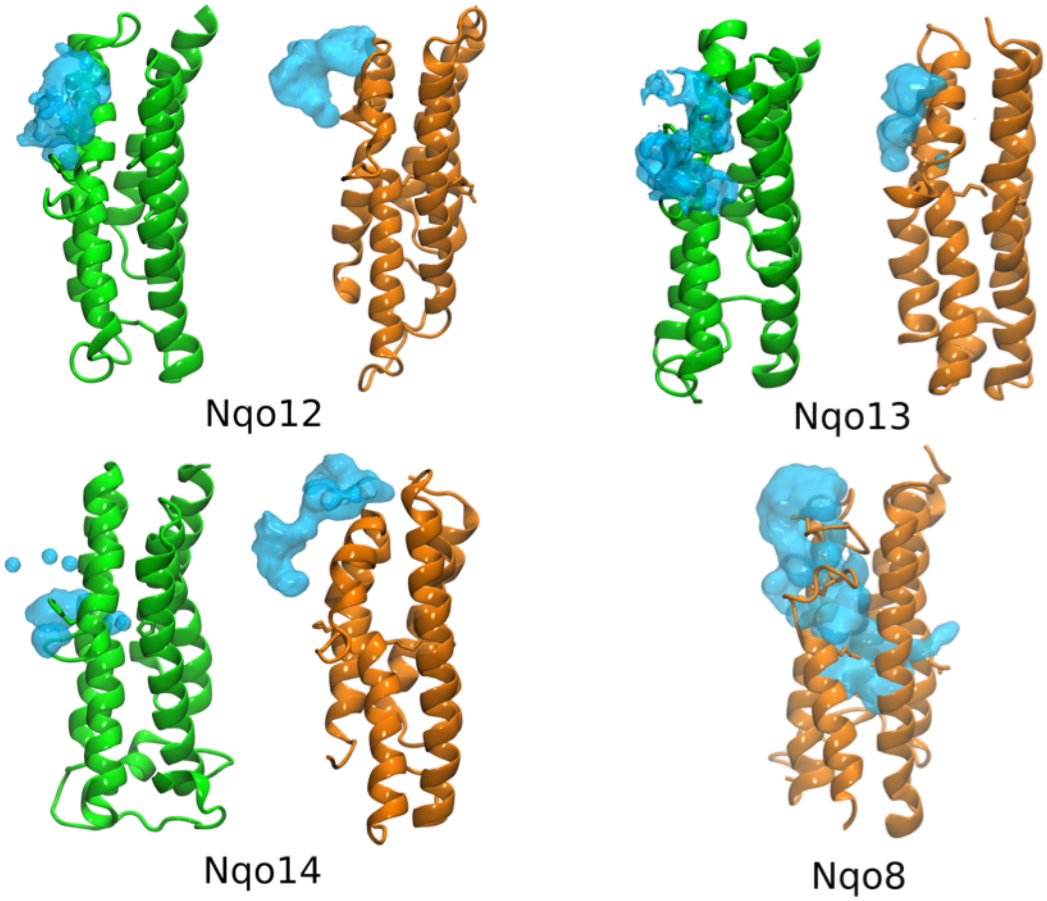

Fig. S1. The structure and hydration patterns of TM4-8/9-13 in the antiporter-like subunit (orange and green) and TM2-6 of Nqo8 subunit (orange). The volumetric water occupation maps are shown in light blue. Hydration pattern show similarities in all subunits. TM9-13 (green) and TM2-6 of Nqo8 (orange) have been rotated by 180 degrees for visual clarity.

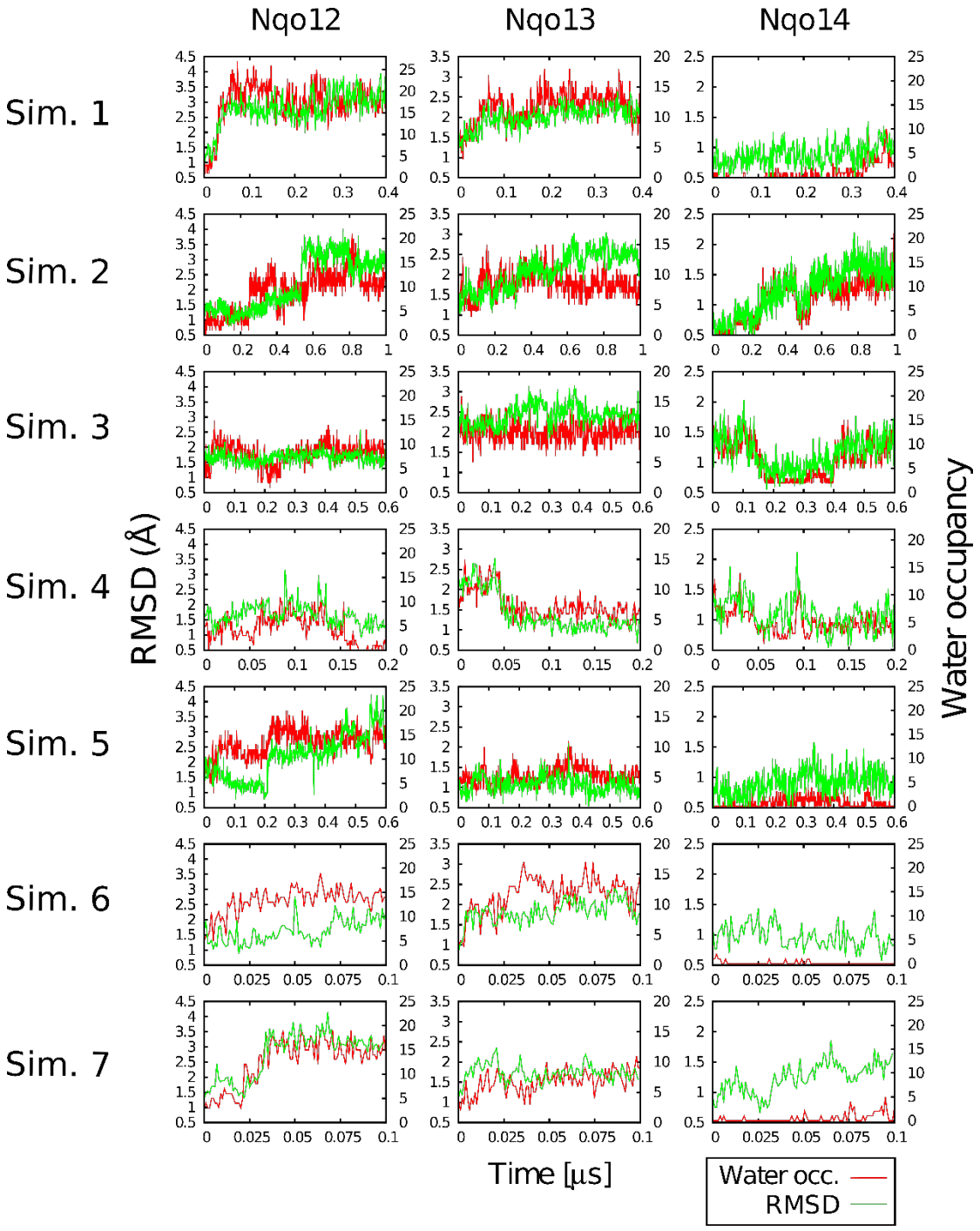

Fig. S2. The correlation between the root-mean-square-deviation (RMSD) of the broken helix elements (TM7b) in simulations **1-7** (Table S1) and the water occupancy in the N-side channel for Nqo12-14. The RMSD of the broken helices has been calculated relative to the X-ray structure (PDB ID: 4HEA) by aligning each subunit individually.

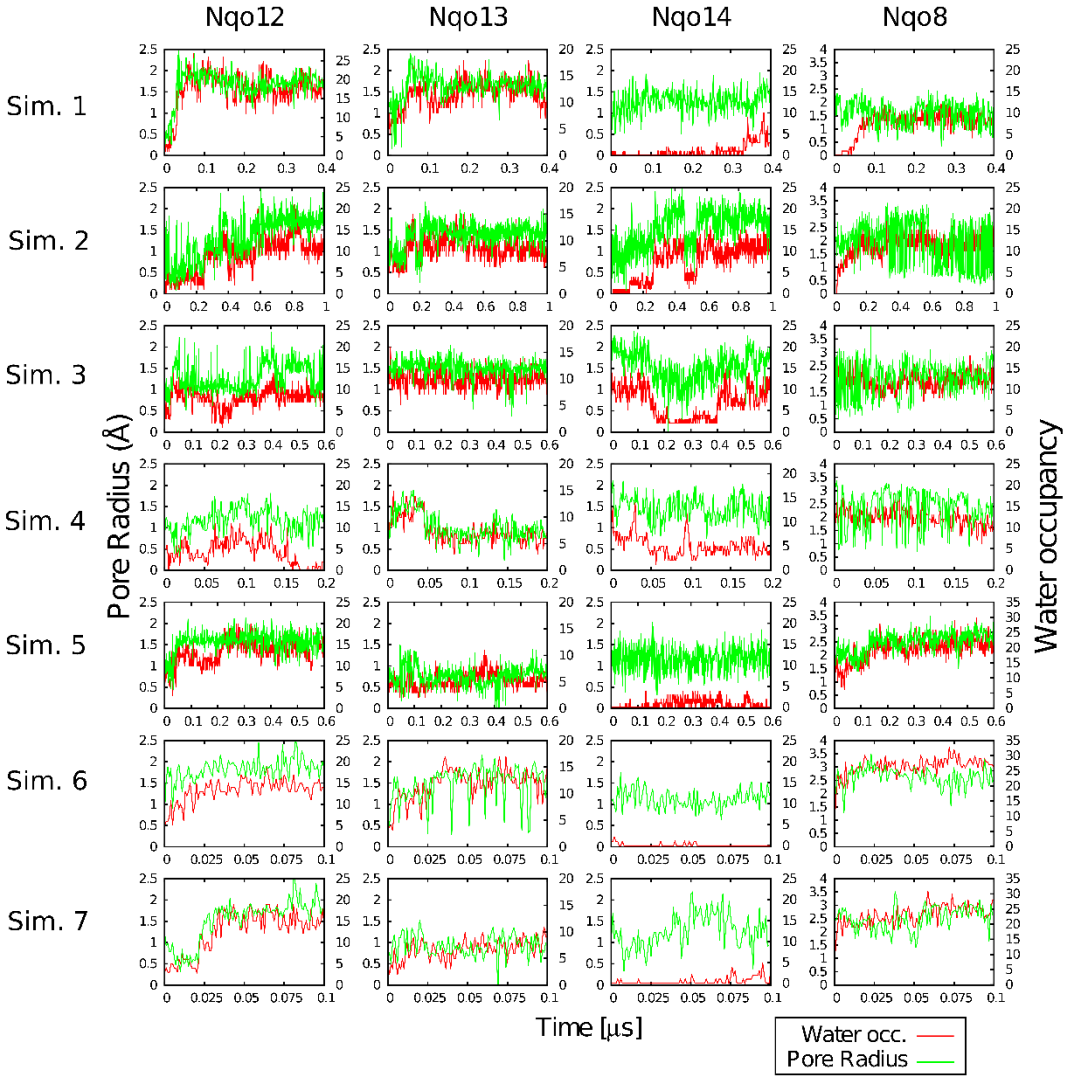

Fig. S3. The pore radius and the water occupancy of the N-side channel in simulations **1-7** (Table S1) for Nqo12-14 and Nqo8. Pore radii are calculated using the HOLE software.

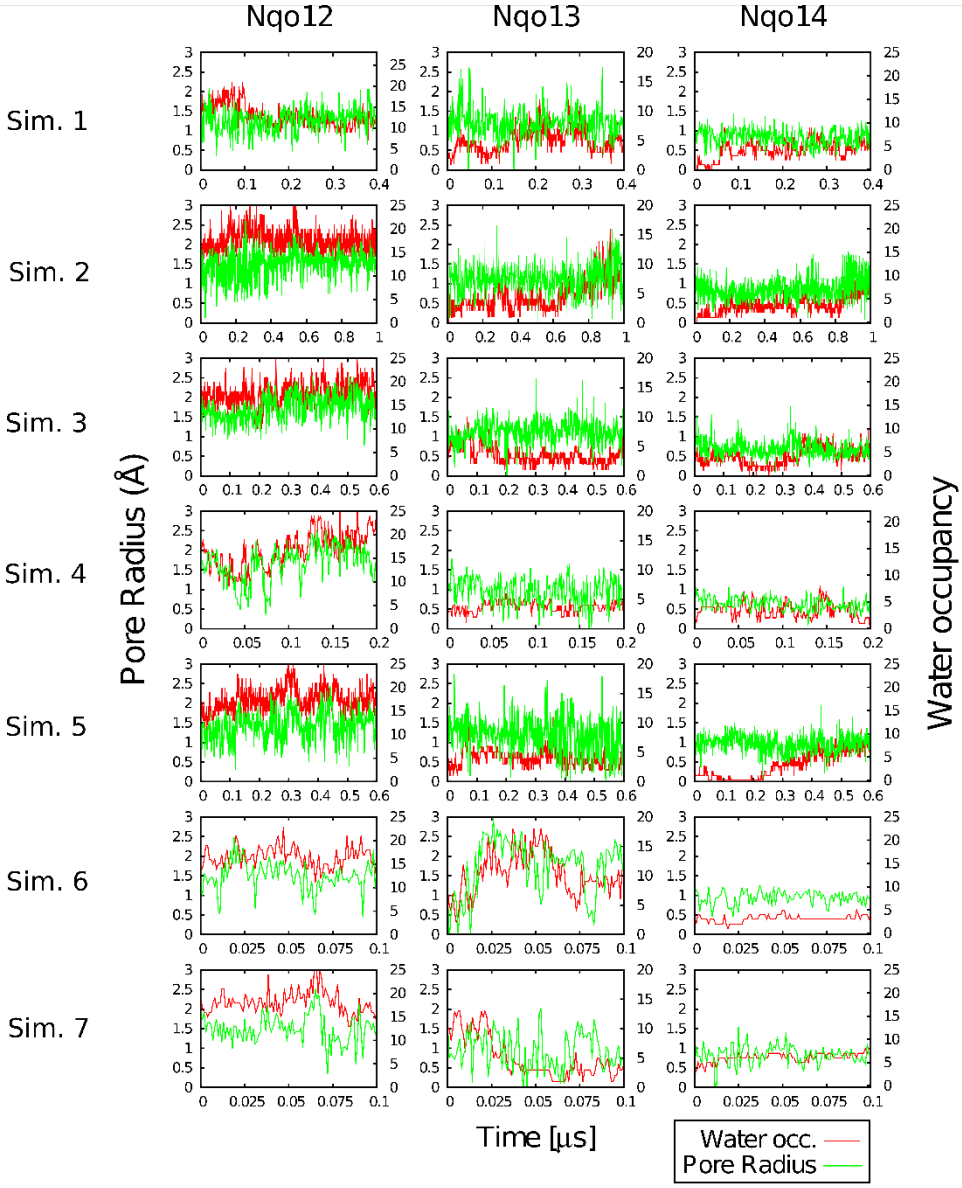

Fig. S4. The pore radius and the water occupancy of the P-side channel in simulations **1**-**7** (Table S1) for Nqo12-14. Pore radii are calculated using HOLE software.

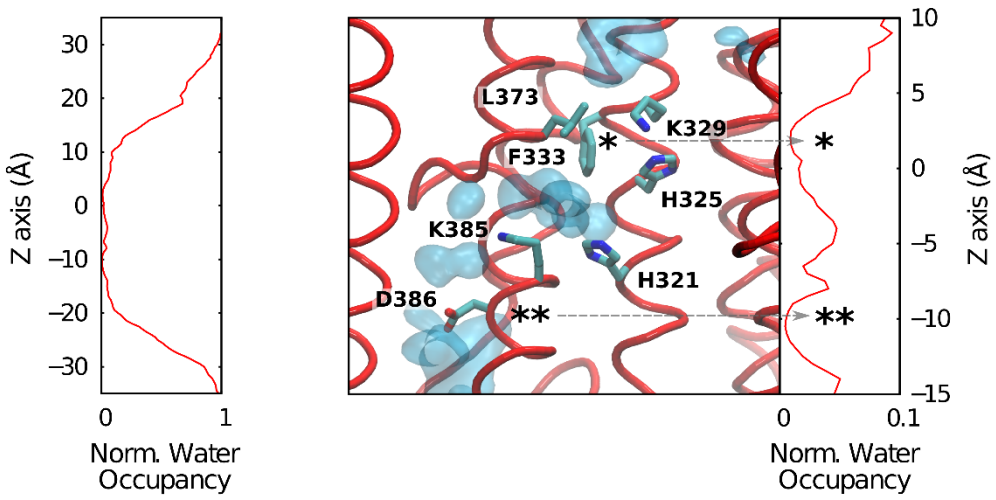

Fig. S5. ***Left***: Water occupancy along the membrane normal (z-axis) in Nqo12. ***Right***: The putative hydrophobic gate in Nqo12. Leu-373 and Phe-333 (shown in sticks) block the water connectivity (in blue surfaces) from the N-side, in the region between Lys-329 and Lys-345, while Asp-386 blocks the connectivity to the P-side. *Inset*: Water occupancy along the membrane normal (z-axis) inside the subunit. Water molecules around 5 Å from residues aligning the channel were selected for the occupancy calculations.

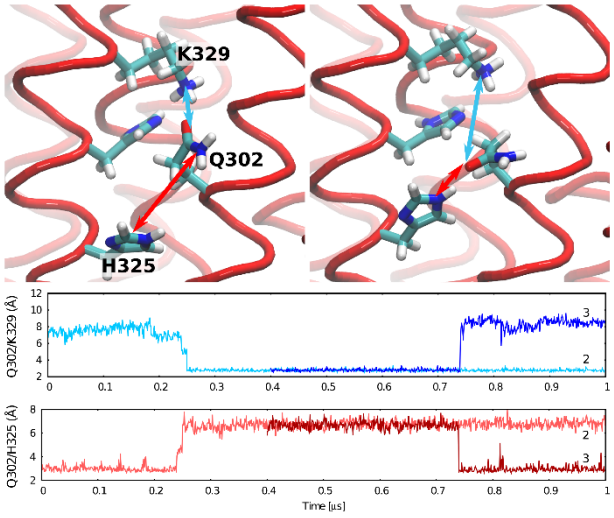

Fig. S6. The distance between Gln-302$_{12}$/Lys-329$_{12}$ (light and dark blue) and Gln-302$_{12}$/His-325$_{12}$ (light and dark red) in simulations **2** and **3**, showing that the sidechain of the Gln-302 switches contacts between Lys-329 and His-325.

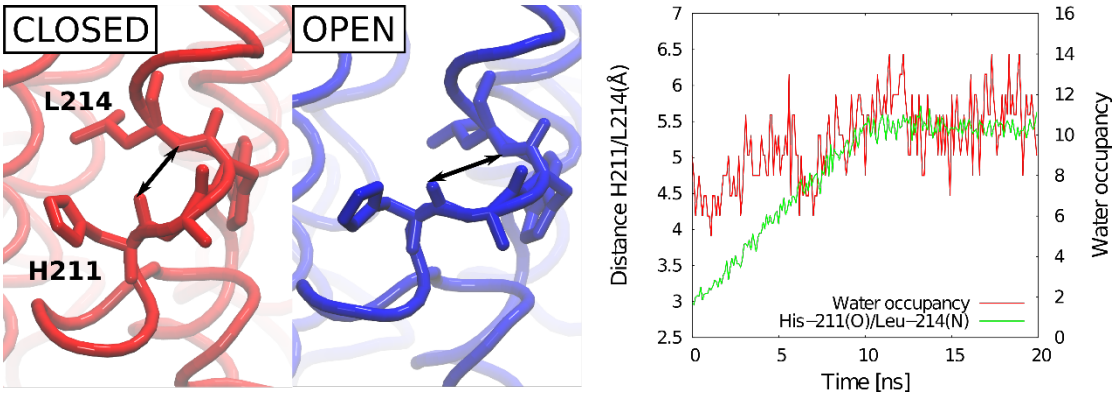

Fig. S7. ***Left*:** the distance of the backbone-backbone hydrogen bond between Leu-214_{13} and His-211_{13} at the tip of the broken helix TM7b in subunit Nqo13 was used as a reaction coordinate in the steered molecular dynamics (SMD) simulations. ***Right*:** Correlation between the channel opening (red trace) and channel hydration (green trace) obtained from SMD simulations.

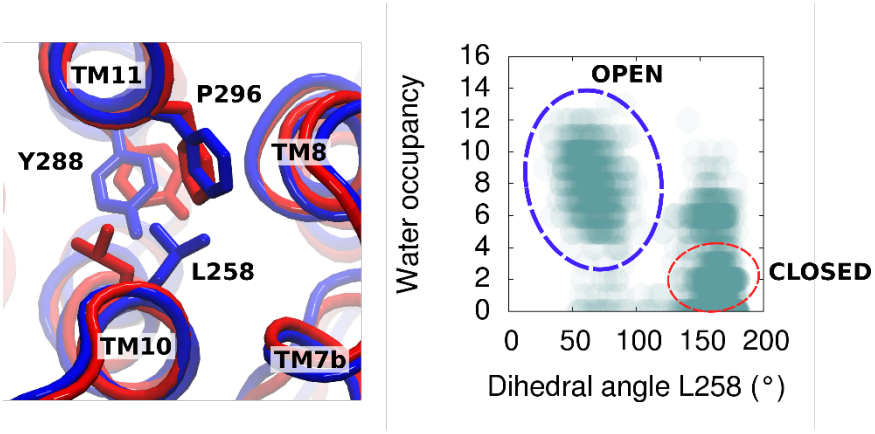

Fig. S8. ***Left*:** Closed channel (in red) and open channel (in blue) suggest that the sidechain of Leu-258 undergoes a conformational change during the channel opening/closure. ***Right***: The water occupancy within the channel correlates with the sidechain orientation (dihedral angle) of Leu-258.

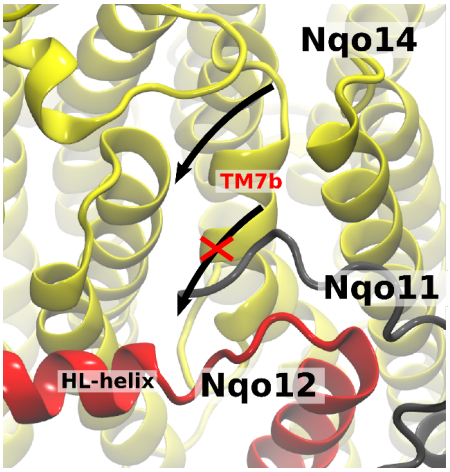

Fig. S9. The C-terminal loop of Nqo11 (in grey) reduces water accessibility to Nqo14 (in yellow) at the location where the channel forms in Nqo13 (crossed arrow), near the HL-helix (in red). The channel is observed near the TM7b broken helix, in similar position to the N-side water pathway in Nqo12 (arrow).

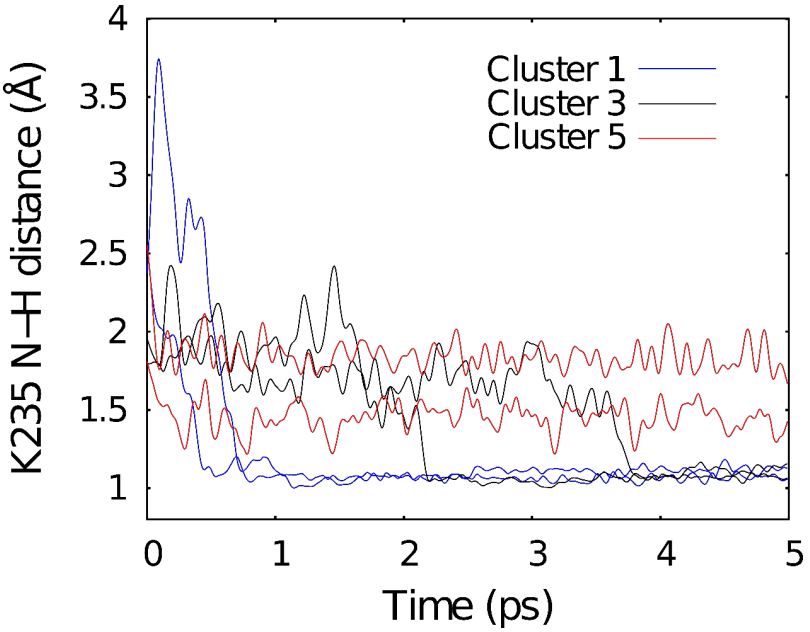

Fig. S10. Distance between the nitrogen atom of Lys-235 (NZ) and the hydrogen atom of the closest water molecule from different classes (see Table S5). The proton transfer proceed fast when the hydrogen-bonded network is formed (class 1), requires a longer reorganization time if partially broken (class 3), and occurs less frequently if the network is completely broken/channel closed (class 5).

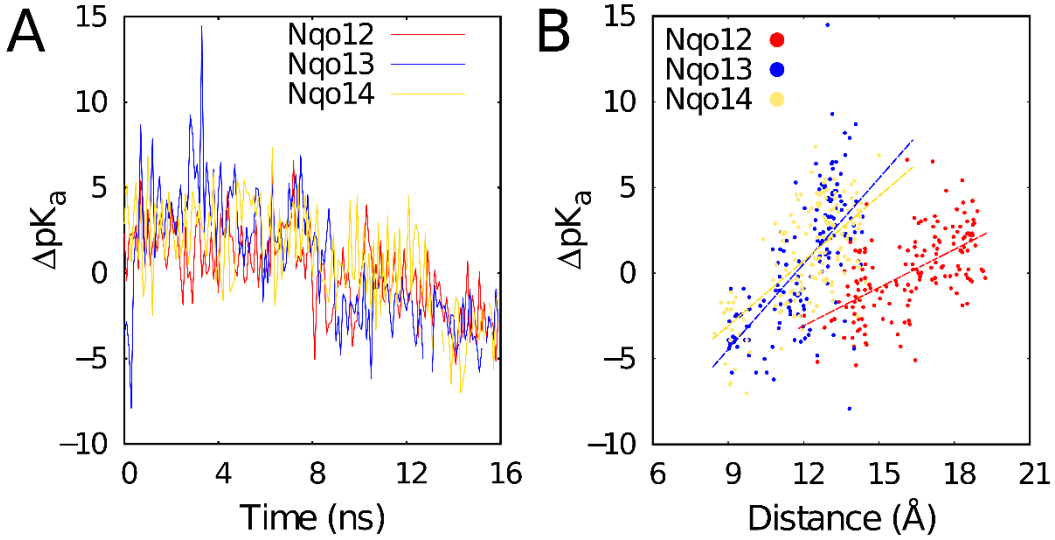

Fig. S11. (A) pK_a shifts of $Lys329_{12}$/$Lys235_{13}$/$Lys216_{14}$ during SMD simulations (see Table S1) of the three antiporter-like subunits. Comparison of subunit Nqo12 (blue), Nqo13 (red) and Nqo14 (yellow) shifts suggest similar effects of the dissociation of the K/E pairs. Calculated pK_a (see Methods) have been shifted by their average values during the trajectory ($Lys329_{12}$ = 16.2 , $Lys235_{13}$ = 13.7, $Lys216_{14}$ = 47.8) **(B)** Correlation of Lys-Lys ($Lys329_{12}$/$Lys216_{12}$ – $Lys235_{13}$/$Lys204_{13}$ - $Lys216_{14}$/$Lys186_{14}$) distances and pK_a shifts of $Lys329_{12}$/$Lys235_{13}$/$Lys216_{14}$ during SMD dynamics. The middle Lys is modeled in the protonated states during the SMD simulations (Table S1).

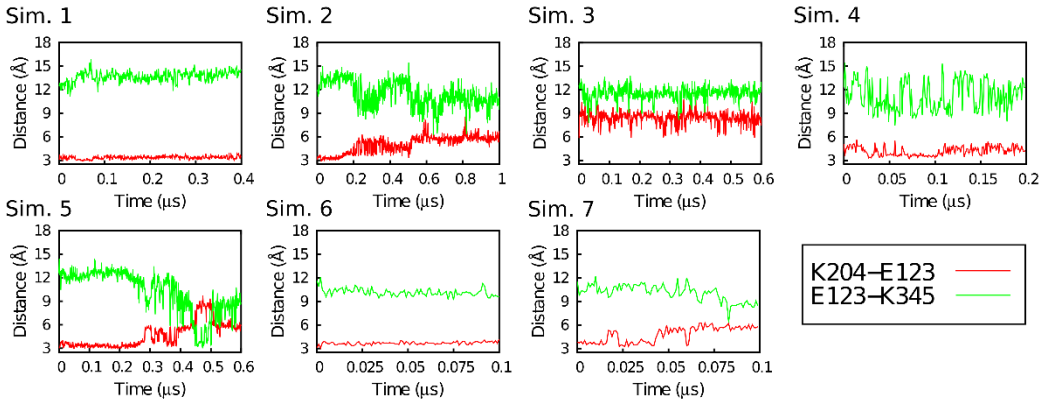

Fig. S12. Dynamics of salt-bridges between Lys-204_{13}/Glu-123_{13} (top) and Lys-345_{14}/Glu-123_{13} (bottom) pairs in Simulations **1-7.**

SI Table S1. Summary of MD simulation setups.

Simulation	Length (ns)	Initiated from	Comment
1	400	X-ray after equilibration	PB titration at 100 ns and 200 ns
2	1000	X-ray after equilibration	PB titration at 100 ns and 200 ns
3	600	after 400 ns of Simulation 2	deprotonated:$K216_{12}$, $K204_{13}$, $K186_{14}$, protonated: $D166_{12}$ $E123_{13}$, $E112_{14}$
4	200	after 400 ns of Simulation 2	deprotonated: $K329_{12}$, $K385_{13}$, $K235_{13}$, $K345_{14}$, $K216_{14}$, $H211_{13}$ protonated: $E377_{13}$
5	600	X-ray after equilibration	-
6	100	X-ray after equilibration	-
7	100	X-ray after equilibration	-
8	20	after 200 ns of Simulation 2	SMD on $H211_{13}$/$L214_{13}$
9	16	after 600 ns of Simulation 5	SMD on $K216_{12}$/$D166_{12}$, constrained position of D166
10	16	after 600 ns of Simulation 5	SMD on $K204_{13}$/$E123_{13}$
11	16	after 400 ns of Simulation 2	SMD on $K186_{14}$/$E112_{14}$
12	350	25 frames of Simulation 9	REUS on $K204_{13}$/$E123_{13}$, Lys-235_{13} in protonated state
13	350	25 frames of simulation 9	REUS on $K204_{13}$/$E123_{13}$, Lys-235_{13} in neutral state
Total	**3768**		

Table S2. Protonation states of titratable residues along the conserved chain in subunits Nqo7/8/11/12/13/14 in the MD simulations 1-7. HSE - ε-protonated His; HSD - δ-protonated His; HSP - doubly protonated His. All other His residues are δ-protonated, if not otherwise states. QH_2 - quinol; Q - quinone. Ox - N2 oxidized state; red – N2 reduced state. All other cofactors are in the oxidized state.

Residue	**1**	**2**	**3**	**4**	**5**	**6**	**7**
K385$_{12}$	+1	+1	+1	0	+1	+1	+1
H241$_{12}$	HSE	HSE	HSE	HSE	HSE	HSD	HSD
H321$_{12}$	HSE	HSE	HSE	HSE	HSE	HSD	HSD
H325$_{12}$	HSD	HSD	HSD	HSD	HSD	HSD	HSD
K329$_{12}$	+1	+1	+1	0	+1	+1	+1
K216$_{12}$	+1	+1	0	+1	+1	+1	+1
D166$_{12}$	-1	-1	0	-1	-1	-1	+1
E377$_{13}$	0	0	0	-1	-1	-1	-1
H292$_{13}$	HSE	HSE	HSE	HSE	HSD	HSD	HSD
K235$_{13}$	+1(0-100 ns)	+1	+1	0	+1	+1	+1
K204$_{13}$	+1	+1	0	+1	+1	+1	+1
E123$_{13}$	-1	-1	0	-1	-1	-1	-1
H211$_{13}$	HSP	HSP	HSP	HSD	HSE	HSD	HSD
K345$_{14}$	+1	+1	+1	0	+1	+1	+1
H265$_{14}$	HSE	HSE	HSE	HSE	HSD	HSD	HSD
K216$_{14}$	+1	+1	+1	0	+1	+1	+1
K186$_{14}$	+1	+1	0	+1	+1	+1	+1
E112$_{14}$	-1	-1	0	-1	0	-1	-1
E67$_{11}$	0	0	0	0	-1	-1	-1
E32$_{11}$	0	0	0	0	-1	-1	-1
D72$_{7}$	0	0	0	0	0	-1	-1
E74$_{7}$	0	0	0	0	-1	-1	-1
E130$_{8}$	0	0	0	0	-1	-1	-1
E163$_{8}$	-1	-1	-1	0	0	-1	-1
E213$_{8}$	0	0	0	0	-1	-1	-1
E248$_{8}$	-1	-1	-1	-1	-1	-1	-1
E223$_{8}$	-1	-1	-1	-1	-1	-1	-1
E225$_{8}$	-1	-1	-1	-1	-1	-1	-1
E227$_{8}$	0	0	0	0	-1	-1	-1
Quinone	Q	QH_2	QH_2	QH_2	Q	Q	Q
FeS (N2)	red	Ox	ox	ox	red	ox	ox

Table S3. Conserved residues observed along the water channels from the N- and P-sides of the membrane in the MD simulations. Residues with identified influence on the activity are marked in red. Residues marked with asterisk are likely to be involved in the proton transfer reaction.

Nqo12	Asp-70, Asp-122, Glu-132, Lys-157, Arg-163, Asp-166, Lys-216, Met-223, Trp-225, Met-230, Pro-233, Thr-234, Ser-237, Ala-238, His-241, Thr-276, Asp-290, Ile-291, Lys-292, Lys-293, Val-295, Ala-296, Ser-298, Thr-299, Ser-301, Gln-302, Tyr-305, His-321*, His-325*, Phe-328, Lys-329*, Leu-332, Ile-340, Asp-348, Arg-350, Leu-373, Phe-382, Trp-383, Lys-385*, Asp-386*, Leu-389, Thr-413, Tyr-416, Arg-419, Phe-425
Nqo13	Asp-68, Asp-114, Glu-123, Thr-147, Lys-204, Pro-206, His-211*, Trp-213, Leu-214, Pro-215, Pro-216, His-218, Gln-219, Glu-220, Thr-232, Lys-235*, Arg-243, Leu-263, Tyr-270, Lys-282, Thr-283, Ala-286, Tyr-287, Leu-290, Ser-291, His-292*, Met-293, Ser-318, Thr-322, Leu-325, Phe-326, Arg-335, Leu-339, Pro-369, Phe-374, Glu-377*, Phe-378, Leu-381, Tyr-405*
Nqo14	Met-1, Gln-60, Glu-83, Glu-112, Gln-128, Glu-131, Lys-135, Phe-137, Lys-186, His-193, Trp-195, Asp-198, Gln-200, Thr-205, Lys-216*, Gln-251, Lys-255, Arg-256, Leu-258, Tyr-260, Ser-261, Ser-262, His-265*, Tyr-268, Tyr-284, Tyr-288, Phe-296, Ser-332, Leu-333, Ile-336, Pro-337, Gly-341, Phe-342, Phe-349, Lys-345*, Ser-368, Tyr-374, Tyr-375
Nqo8	Leu-15, Glu-35, Arg-36, Arg-45, Asn-49, Asp-62, Glu-130, Tyr-134, Ser-161, Tyr-162, Glu-163*, Glu-213*, Arg-216, Pro-218, Phe-219, Asp-220, Pro-222, Glu-223*, Glu-225*, Glu-227*, Leu-228, Ser-237, Glu-248, Tyr-249, Arg-299, Arg-301, Arg-305

Table S4. Residue modeled in the QM region in the QM/MM MD simulations. To model the broken water connectives from the N-side in eight simulations of setup 1, QM region comprises also Glu-557_{12}, Tyr-287_{13}, Tyr-270_{13}.

. **Name**	**QM Setup**	**Simulation time**
Setup 1	His-211 (δ-state), His-218 (δ-state), Lys-235 (neutral), Thr-232.	64 x 5 ps
Setup 2	His-218 (δ-state), Lys-235 (protonated), His-292 (δ-state), Thr-322, Glu-377 (deprotonated)	3 x 5 ps

Table S5. Average proton transfer reaction time from independent QM/MM MD simulations. The simulations are classified according to the maximum distance of heavy atom along the water wire in the starting structure of the simulation. Percentage of proton transfer ($\%_{\mathbf{pT\ obs.}}$) is calculated by dividing the number of simulation in which the pT is observed by the total number of simulation for each cluster ($N_{\mathbf{tot}}$). Average of pT time ($\bar{t}$) is obtained by assigning a value of 5 ps (maximum simulation length) for each simulation in which the pT was not observed

Class	Max ($\lvert\vec{d}_{\text{acc-don}}\rvert$)	N_{tot}	$\%_{\text{pT obs.}}$	$\bar{t}$ (ps)
1	0<*d*<3.5	11	81%	2.42
2	3.5<*d*<4.5	10	60%	3.16
3	4.5<*d*<5.5	12	33%	3.82
4	5.5<*d*<6.5	14	50%	3.92
5	6.5<*d*	17	41%	4.02

Table S6. pK_a values of conserved charged and polar residues of the membrane domain of complex I calculated using the crystal structure (PDB ID: 4HEA). P and D refer to protonated and deprotonated residues in the pH range below 0 and above 20.

Residue	pK_a	Residue	pK_a	Residue	pK_a
K385$_{12}$	18.9	**E123$_{13}$**	9.2	**D72$_{7}$**	P
K329$_{12}$	18.5	**H211$_{13}$**	11.3	**E74$_{7}$**	P
K216$_{12}$	1.2	**K345$_{14}$**	22.5	**E130$_{8}$**	P
D166$_{12}$	P	**K216$_{14}$**	7	**E163$_{8}$**	P
E132$_{12}$	D	**K186$_{14}$**	D	**E213$_{8}$**	P
E377$_{13}$	17.1	**E112$_{14}$**	P	**E248$_{8}$**	2.3
K235$_{13}$	8.1	**E67$_{11}$**	P	**E223$_{8}$**	D
K204$_{13}$	D	**E32$_{11}$**	2.4	**E225$_{8}$**	D
E227$_{8}$	P				

Table S7. Selection of residue used for selection of water molecules shown in Fig. 2.; residues labeled in red were used for calculation of water occupancies in Fig. 3, Fig. S2, Fig. S3, and Fig. S4 by searching for water molecules located within a radius of 4-5 Å from these residues.

Nqo12	Asp-166, Lys-216, Glu-132, Arg-163, Val-295, His-321, His325, Lys-329, Phe-333, Lys-385, Asp-386, Ala-390, Phe-425
Nqo13	Glu-123, Lys-204, Leu-214, Pro-215, Lys-235, His-292, Gly-370, Glu-377, Val-445
Nqo14	Leu-258, Lys-216, His-265, Phe-296, Pro-338, Phe-342, Trp-343, Lys-345, Leu-414
Nqo11	Glu-32, Glu-67
Nqo7	Glu-72
Nqo8	Glu-130, Glu-213, Glu223, Glu-163